

StochGradAdam: Accelerating Neural Networks Training with Stochastic Gradient Sampling

Juyoung Yun

Department of Computer Science
Stony Brook University
juyoung.yun@stonybrook.edu

Abstract

In the rapidly advancing domain of deep learning optimization, this paper unveils the StochGradAdam optimizer, a novel adaptation of the well-regarded Adam algorithm. Central to StochGradAdam is its gradient sampling technique. This method not only ensures stable convergence but also leverages the advantages of selective gradient consideration, fostering robust training by potentially mitigating the effects of noisy or outlier data and enhancing the exploration of the loss landscape for more dependable convergence. In both image classification and segmentation tasks, StochGradAdam has demonstrated superior performance compared to the traditional Adam optimizer. By judiciously sampling a subset of gradients at each iteration, the optimizer is optimized for managing intricate models. The paper provides a comprehensive exploration of StochGradAdam’s methodology, from its mathematical foundations to bias correction strategies, heralding a promising advancement in deep learning training techniques.

1 Introduction

Deep learning, with its ability to model complex relationships and process vast amounts of data, has revolutionized various fields from computer vision to natural language processing [11, 20]. The heart of deep learning lies in the optimization algorithms that tune model parameters to minimize loss and increase accuracy [28]. The choice of an optimizer can significantly influence a model’s convergence speed, final performance, and overall stability [3]. In this rapidly evolving arena, we continuously strive for more efficient and powerful optimization techniques.

In our pursuit of advancing optimization methodologies, our focus extends beyond merely the architectural intricacies of models. Instead, we place significant emphasis on the mechanisms governing weight updates during the training phase. Renowned optimization algorithms such as Adam [17], RMSProp [36], and Adagrad [9] have traditionally been the cornerstones that have ushered numerous models to achieve exemplary performance. Yet, the evolving landscape of deep learning raises a pertinent question: Is there potential to further enhance these optimization strategies, especially when applied to expansive and intricate neural architectures?

To address this query, we introduce StochGradAdam, our novel optimizer that incorporates gradient sampling as a pivotal technique to enhance the accuracy of models. This gradient sampling method not only assists in optimizing the training process but also contributes significantly to the improvement in the model’s generalization on unseen data. In our empirical evaluation, we subject Convolutional Neural Networks (CNNs) like ResNet [14], VGG [32], MobileNetV2[29] and Vision Transformer Model(ViT) [8] to a comprehensive array of tests.

Our examination extends beyond just test accuracy and loss. We delve deeper, investigating the entropy of the class predictions. Entropy, in this context, measures the uncertainty in the model’s

GitHub repository will be accessed at:

predictions across classes [7]. A model with lower entropy exudes confidence in its predictions, while one with higher entropy reflects greater uncertainty. By harnessing the strength of StochGradAdam with gradient sampling, we have observed a decrease in entropy, indicating a more confident prediction by the models. Through studying entropy, we strive to gain a more nuanced understanding of the model’s behavior, shedding light on aspects that might remain obscured when solely relying on traditional metrics [38].

Algorithm 1 StochGradAdam, a modified version of the Adam optimizer with random gradient sampling. See section 3 for details explanation for the algorithm of our proposed optimizer.

Require: Stepsize (Learning rate) α
Require: Decay rates $\beta_1, \beta_2 \in [0, 1)$ for the moment estimates
Require: Stochastic objective function $f(\theta)$ with parameters θ
Require: Initial parameter vector θ_0
Require: sampling rate s

- 1: Initialize m and v as zero tensors ▷ Moment vectors
- 2: **while** θ not converged **do**
- 3: Get gradient g with respect to the current parameters θ
- 4: Generate a random mask $mask$ with values drawn uniformly from $[0, 1]$
- 5: $grad_mask \leftarrow mask < s$ ▷ Mask gradient based on sampling rate
- 6: $grad_sampled \leftarrow \text{where}(grad_mask, g, 0)$
- 7: $\beta_{1_t} \leftarrow \beta_1 \times \delta$
- 8: $m_t \leftarrow \beta_{1_t}m + (1 - \beta_{1_t})grad_sampled$
- 9: $v_t \leftarrow \beta_2v + (1 - \beta_2)grad_sampled^2$
- 10: $m_{corr_t} \leftarrow \frac{m_t}{1 - \beta_1^{t+1}}$
- 11: $v_{corr_t} \leftarrow \frac{v_t}{1 - \beta_2^{t+1}}$
- 12: $\theta \leftarrow \theta - \alpha \frac{m_{corr_t}}{\sqrt{v_{corr_t} + \epsilon}}$
- 13: Update m with m_t and v with v_t
- 14: **end while**
- 15: **return** θ ▷ Updated parameters

Following these findings, we further elucidate the contribution of StochGradAdam. This optimizer results from rigorous research and embodies state-of-the-art algorithmic principles. Preliminary results suggest that StochGradAdam exhibits performance on par with, if not superior to, existing optimization methods. A detailed explanation of the algorithm and its update rule is provided in section 3.

2 Related Works

The exploration of gradient-based optimization techniques has been a cornerstone in deep learning research. Over the years, this has given rise to various methodologies that aim to harness the power of gradients in more effective ways. Among them, gradient sampling and techniques with similar goals have piqued the interest of researchers, leading us on a more exhaustive dive into the landscape.

Stochastic Gradient Descent (SGD) serves as the foundation for many gradient-based methods. It updates the model’s parameters using only a subset of the entire dataset. This inherent introduction of noise is balanced well with computational efficiency and commendable convergence properties [3].

Delving deeper into gradient behavior, Sparse Gradients Techniques emerged from observations that many gradient components might be trivial for model updates despite their existence. Such techniques, therefore, prioritize gradients that exceed certain thresholds, aiming for updates that are sparser yet potentially more informative [39].

Adaptive Sampling techniques, an evolution in gradient sampling, tailor the subset of gradients under consideration by observing the gradients’ historical behavior. These techniques operate under the hypothesis that gradients showing significant fluctuations over time might be more pivotal for efficient optimization [42]. Gradient Sampling Methods[6] for Nonsmooth Optimization offer a distinct approach, especially beneficial for tackling nonsmooth problems. They rely on the concept of

randomly sampling gradients, a strategy particularly beneficial when the gradient might be challenging to compute or might not exist at all.

The RSO (random search optimization) technique by Tripathi and Singh[37] offers a unique perspective on optimization. Instead of relying on direct gradient computations, RSO introduces perturbations to weights and evaluates their impact on the loss function. This approach becomes particularly beneficial in situations where computing the gradient is either intricate or entirely unfeasible. The essence of RSO underscores the notion that for certain problems, venturing into the vicinity of randomly initialized networks without the need for exact gradient computations can be sufficient for optimization. Contrastingly, the StochGradAdam method amalgamates the principles of Gradient Sampling with the renowned ADAM optimizer. While both RSO and Gradient Sampling diverge from traditional gradient-based methods, StochGradAdam’s approach is distinct. It capitalizes on gradient information, even if it’s sampled, to guide the optimization process. This gradient-centric nature of StochGradAdam allows it to potentially provide more precise weight adjustments. The key differentiation between RSO and StochGradAdam lies in their treatment of gradients: while RSO bypasses them in favor of random perturbations, StochGradAdam harnesses sampled gradients to inform its optimization steps.

In this rich tapestry of gradient-based methodologies, our StockGradAdam emerges with distinction. Instead of merely adopting the usual random sampling approach, our method pulsates with adaptive intelligence. It aligns with the training phase’s nuances and the inherent gradient variances, balancing exploration and exploitation. Furthermore, its standout feature lies in the harmonious melding of gradient sampling with momentum intricacies. This symbiosis magnifies the collective strengths of both strategies. Moreover, our technique adeptly navigates the terrain of sparse gradients, ensuring precision with each update. The vast landscape of gradient manipulation methods might seem saturated at first glance. However, the introduction and success of StockGradAdam reiterate that there’s always room for innovative, impactful strategies in gradient-based optimizations.

3 Methodology: StochGradAdam Optimizer

The StochGradAdam optimizer is an extension of the Adam optimizer [17], incorporating selective gradient sampling to bolster optimization efficacy. Its principal update rule is:

$$\mathbf{w}_{t+1} = \mathbf{w}_t - \alpha \frac{m_{\text{corr}_t}}{\sqrt{v_{\text{corr}_t} + \epsilon}}, \quad (1)$$

where α symbolizes the learning rate, m_{corr_t} is the bias-corrected moving average of the gradients, and v_{corr_t} is the bias-corrected moving average of the squared gradients. The following sections elaborate on the inner workings of this formula.

3.1 Preliminaries

Let a trainable parameter be denoted as $\mathbf{w} \in \mathbb{R}^d$, where \mathbb{R}^d is the space of all possible parameters. The optimizer maintains two state variables for each such parameter:

$m(\mathbf{w})$: Moving average of the gradients with respect to \mathbf{w} .

$v(\mathbf{w})$: Moving average of the squared gradients with respect to \mathbf{w} .

Furthermore, the hyperparameters are:

$\beta_1, \beta_2 \in (0, 1)$: Exponential decay rates.

$\text{decay} \in \mathbb{R}^+$: Decay multiplier for β_1 .

$s \in (0, 1)$: Probability for gradient sampling.

$\epsilon \in \mathbb{R}^+$: Constant ensuring numerical stability.

3.2 Gradient Sampling

Gradient sampling, in the context of optimization, is a technique where a subset of the gradients is randomly selected during the optimization process. This method not only promotes more robust training by sifting through gradient components, potentially reducing the influence of noisy or outlier

data, but also enhances the exploration of the loss landscape, leading to more reliable convergence. Additionally, our approach to gradient sampling is designed to adaptively choose the sampling rate based on training dynamics, ensuring that more relevant gradients are considered during pivotal training phases.

3.2.1 Stochastic Mask Generation

Given a gradient \mathbf{g} , the objective is to determine whether each component of this gradient should be considered in the update. To this end, a stochastic mask Ω is introduced. Each component of Ω is independently derived by drawing from the uniform distribution $\mathcal{U}(0, 1)$:

$$\Omega_i = \begin{cases} 1 & \text{if } \mathcal{U}(0, 1) < s, \\ 0 & \text{otherwise,} \end{cases} \quad (2)$$

for $i = 1, 2, \dots, d$, where d represents the dimensionality of \mathbf{g} . Here, $\mathcal{U}(0, 1)$ denotes a uniform random variable over the interval $[0, 1]$, and s is a predefined threshold dictating the average portion of gradients to be sampled.

3.2.2 Computing the Sampled Gradient

With the stochastic mask in hand, the next objective is to compute the sampled gradient, denoted by ϕ . This is accomplished by executing an element-wise multiplication between \mathbf{g} and Ω :

$$\phi_i = \Omega_i \times g_i, \quad (3)$$

for $i = 1, 2, \dots, d$. Thus, we get:

$$\phi = \Omega \odot \mathbf{g}, \quad (4)$$

where \odot signifies element-wise multiplication, ensuring only the components of the gradient flagged by Ω influence the sampled gradient.

The underlying idea of gradient sampling is rooted in the belief that not all gradient components are equally informative. By stochastically selecting a subset, one can potentially accelerate the optimization process without sacrificing much in terms of convergence properties. Moreover, this also introduces a form of noise, which can, in some cases, assist in escaping local minima or saddle points in the loss landscape.

3.3 State Updates

The StochGradAdam optimizer maintains two state variables, m and v , representing the moving averages of the gradients and their squared values, respectively. Their iterative updates are influenced by the gradient information and specific hyperparameters.

3.3.1 Moving Average of Gradients: m

The moving average of the gradients, m , is updated through an exponential decay mechanism. At each iteration, a part of the previous moving average merges with the current sampled gradient:

$$m_t = \beta_1^t m + (1 - \beta_1^t) \phi, \quad (5)$$

Here, β_1 signifies the exponential decay rate for the moving average of the gradients [17]. The term β_1^t showcases the adjusted decay rate at the t^{th} iteration, defined as:

$$\beta_1^t = \beta_1 \times \text{decay}. \quad (6)$$

The function of β_1 is to balance the memory of past gradients. A value nearing 1 places more emphasis on preceding gradients, yielding a smoother moving average. Conversely, a value nearing 0 focuses on the recent gradients, making the updates more adaptive [28].

3.3.2 Moving Average of Squared Gradients: v

Similarly, v captures the moving average of the squared gradients. It's updated as:

$$v_t = \beta_2^t v + (1 - \beta_2^t) \phi \odot \phi, \quad (7)$$

Here, β_2 denotes the exponential decay rate for the moving average of squared gradients [17]. Analogous to β_1 but for squared values, β_2^t is the adjusted decay rate at the t^{th} iteration, defined as:

$$\beta_2^t = \beta_2 \times \text{decay}. \quad (8)$$

The element-wise multiplication \odot ensures that each gradient component's squared value is computed individually [2].

3.4 Bias Correction

Given the nature of moving averages, especially when initialized with zeros, the early estimates of m and v can be significantly biased towards zero. To address this, bias correction is employed to adjust these moving averages [17].

3.4.1 Correcting the Bias in m

The bias-corrected value of m at the t^{th} iteration is:

$$m_{\text{corr}_t} = \frac{m_t}{1 - \beta_1^t}, \quad (9)$$

Here, the term $1 - \beta_1^t$ serves as a corrective factor to counteract the initial bias [28].

3.4.2 Correcting the Bias in v

Similarly, for v :

$$v_{\text{corr}_t} = \frac{v_t}{1 - \beta_2^t}, \quad (10)$$

This correction ensures that the state variables m and v provide unbiased estimates of the first and second moments of the gradients, respectively [17].

3.5 Parameter Update

StochGradAdam optimizes model parameters by adapting to both the historical gradient and the statistical properties of the current gradient [17]. The update rule for model parameter \mathbf{w}_t at iteration t is:

$$\mathbf{w}_{t+1} = \mathbf{w}_t - \alpha \frac{m_{\text{corr}_t}}{\sqrt{v_{\text{corr}_t} + \epsilon}}, \quad (11)$$

The update can be viewed as an adaptive gradient descent step. By normalizing the gradient using its estimated mean and variance, StochGradAdam effectively scales parameter updates based on their historical and current behavior [2]. StochGradAdam synergizes the principles of stochastic gradient sampling with the Adam optimizer's robustness.

4 Experimental Results

In the subsequent section, we delve into the empirical evaluation of the methodologies discussed thus far. The primary objective of our experiments is to validate the theoretical assertions and gauge the performance of our proposed techniques in real-world scenarios. Through a series of meticulously designed experiments, we compare our methods against established benchmarks, thereby offering a comprehensive assessment of their efficiency, robustness, and scalability. Each experiment is crafted to answer specific questions, shedding light on the strengths and potential limitations of our approach. By coupling rigorous experimental design with diverse datasets and tasks, we aspire to provide readers with a holistic understanding of the practical implications of our contributions.

4.1 Image Classification

4.1.1 CIFAR-10

In the image classification, the accuracy of various deep learning architectures are often deployed to identify the best model for a particular task. This section focuses on the CIFAR-10 dataset[18],

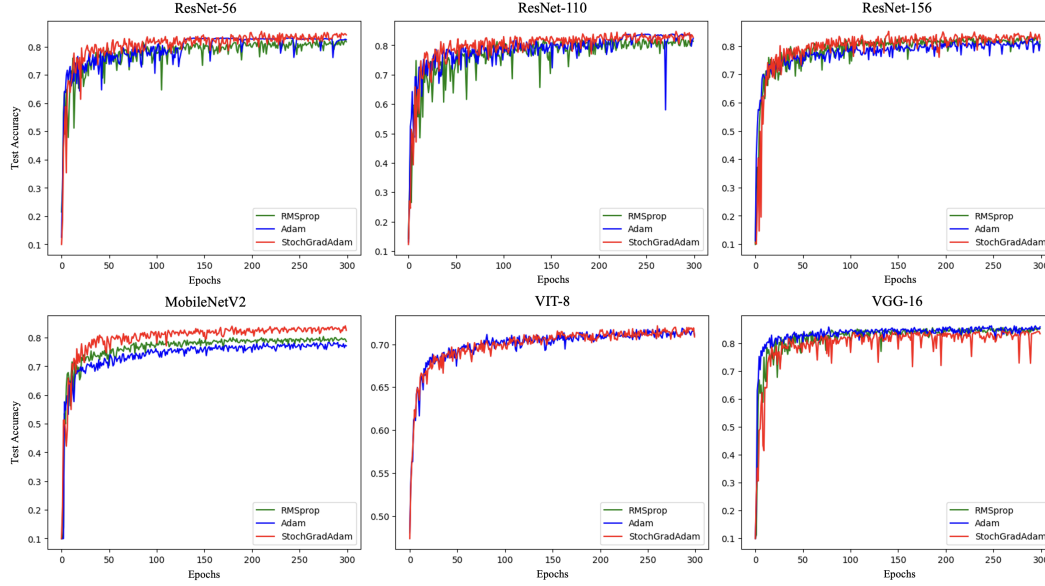


Figure 1: Comparison of test accuracy over 300 epochs on CIFAR-10 dataset for various neural network architectures: ResNet-56, ResNet-110, ResNet-156, MobileNetV2, ViT-8, and VGG-16. Three different optimizers - RMSprop (green), Adam (blue), and StochGradAdam (red) - were used to train each model. The graphs showcase how each architecture and optimizer combination performs over the course of training.

a widely recognized benchmark in the field, to compare the performance of several neural network architectures and optimizers. We train each architecture at a learning rate of 0.01 and implement the model using TensorFlow.

The displayed figure 2 provides a detailed visualization of the test accuracy for various deep learning architectures when trained using different optimizers. Notably, our newly introduced method is depicted in red, distinguishing its performance from the rest.

ResNet-56: Our optimizer manifests a swift uptick in test accuracy during the initial epochs, outpacing other methodologies. Although slight deviations become apparent towards the culmination of training, the overall trend suggests competitive prowess.

ResNet-110: With this architecture in play, our optimizer emulates the trajectory observed in ResNet-56. An impressive ascent during the incipient phases is evident, and despite minor oscillations in later epochs, the optimizer’s performance remains robust.

ResNet-156: This architecture reveals an expeditious surge in test accuracy using our optimizer during the early training, subsequently aligning with trends showcased by other optimizer methodologies.

MobileNetV2: Our optimizer commences with a formidable performance, either paralleling or slightly eclipsing the Adam optimizer across epochs. Despite some intermittent fluctuations, the trend underscores its commendable adaptability to the MobileNetV2 architecture.

ViT-8: Employed on the Vision Transformer model, our optimizer portrays steady advancement in test accuracy, showcasing a consistent and relatively stable performance. The original ViT model was optimized using the Adam method. Notably, when trained with RMSProp at a learning rate of 0.01, the ViT model stagnated, registering a mere 10% test accuracy - reminiscent of random decision-making.

VGG-16: Contrasting the trends observed with other architectures, our optimizer, in tandem with other methods, doesn’t scale to the pinnacle of test accuracy when employed on VGG-16. While the results closely mirror each other across the optimizer spectrum, our method’s performance remains indistinguishable. The rationale for the discernible dip in VGG-16’s performance relative to other

architectures is hypothesized to stem from gradient diminution. This decrease in gradient magnitude can adversely affect gradient sampling.

It's surmised that the unique characteristics of VGG and ViT, particularly in the context of gradient dynamics, might not be optimally suited for our new optimizer. The diminishing gradients observed might be adversely influencing gradient sampling. A more nuanced exploration of this phenomenon and its implications will be delved into within the "Limitation" section of our research.

In summation, our optimizer showcases promising test accuracy metrics across an array of architectures, especially in the nascent training phases. Its rapid convergence coupled with unwavering performance earmarks it as a potent contender for image classification tasks, specifically on the CIFAR-10 dataset

4.2 Segmentation

Following our detailed discussion on classification, we ventured into another pivotal domain of deep learning - segmentation. For our experiments, we adopted the Unet-2 architecture[26] integrated with MobileNetV2 [29], ensuring a balance between computational efficiency and performance. Our optimizer of choice for these experiments was StochGradAdam, running at a learning rate of 0.001.



Figure 2: Comparative visualization of segmentation results on the oxford_iiit_pet dataset using the Unet-2 architecture integrated with MobileNetV2 across different optimizers, including StochGradAdam, Adam, and RMSProp

We sourced our dataset from the renowned oxford_iiit_pet [25], which provides a robust set of images for segmentation tasks. The results of our experiments can be observed in the figure above. A close inspection of the visualizations reveals the strength of our StochGradAdam optimizer. The "Ours Prediction" column demonstrates a more precise and coherent segmentation when compared to other widely-used optimizers like Adam and RMSProp. The boundaries are sharper, and the segmentation masks align more accurately with the true masks, accentuating the prowess of StochGradAdam in driving better model performance.

To conclude, StochGradAdam not only showed promise in the realm of classification but also established its potential in segmentation tasks. Our findings are corroborated by the comparative visual analysis, setting a new benchmark for future optimizers.

5 Analysis: Uncertainty Reduction in Prediction Probabilities

Having observed the performance of various optimizers in our experimental results, one might wonder about the intricacies beyond mere accuracy metrics. The efficacy of an optimizer is not solely gauged by its ability to minimize the loss function but also by its influence on the uncertainty of the model’s predictions. In the realm of deep learning, where models make probabilistic predictions across multiple classes, it’s crucial to delve into how different optimizers shape these probabilities. In this section, we explore the role of optimizers in determining the entropy of prediction probabilities and discuss its implications for uncertainty in predictions.

5.1 Entropy: A Measure of Uncertainty

For a discrete probability distribution $P = (p_1, p_2, \dots, p_n)$, entropy, denoted as $H(P)$, provides a measure of the uncertainty or randomness of the distribution [31]:

$$H(P) = - \sum_{i=1}^n p_i \log(p_i) \quad (12)$$

A distribution that is entirely certain (one probability is 1 and the others are 0) will have an entropy of 0. On the contrary, a uniform distribution, characterized by maximum uncertainty, will possess the highest entropy [7]. To ensure the interpretability and comparability of entropy values, especially when working with distributions over different numbers of outcomes, we resort to normalized entropy [27]:

$$H_{\text{normalized}}(P) = \frac{H(P)}{\log(n)} \quad (13)$$

With this normalization, entropy values are confined between 0 (absolute certainty) and 1 (absolute uncertainty).

5.2 The Role of Optimizers

An optimizer’s main objective is to update model parameters to minimize the associated loss [11]. As this optimization unfolds, the model starts achieving a better fit to the data, leading to predictions marked by heightened confidence [2]. From an entropy perspective, this translates to:

$$H(P_{\text{initial}}) > H(P_{\text{optimized}}) \quad (14)$$

Here, P_{initial} stands for the prediction probabilities before the optimization and $P_{\text{optimized}}$ denotes them post-optimization. The entropy reduction is symbolic of the declining uncertainty in predictions [22].

Different optimizers traverse the parameter space distinctively [28]. While some might directly target the global minima, others might explore the space more expansively. These varied approaches can influence both the rate and magnitude of entropy reduction [17]. To quantitatively gauge the prowess of each optimizer:

$$\Delta H_O = H(P_{\text{initial}}) - H(P_{\text{final}}) \quad (15)$$

A superior value of ΔH_O underlines the optimizer’s proficiency in diminishing prediction uncertainty [40].

5.3 Comparative Visualization: Histograms

For a more intuitive understanding of the influence of different optimizers on prediction uncertainty, we can employ histograms that depict the distribution of normalized entropies subsequent to optimization. This analysis was conducted utilizing TensorFlow, with experiments performed on the ResNet-56[14] architecture applied to the CIFAR-10 dataset[18], all while maintaining a learning rate of 0.01.

The presented figure 3 showcases contrasting characteristics between RMSProp, Adam, and StochGradAdam (Ours) in their approach to prediction uncertainty throughout the epochs. Initially, each optimizer displays a wide distribution in normalized entropy, reflecting a mixture of prediction confidences.

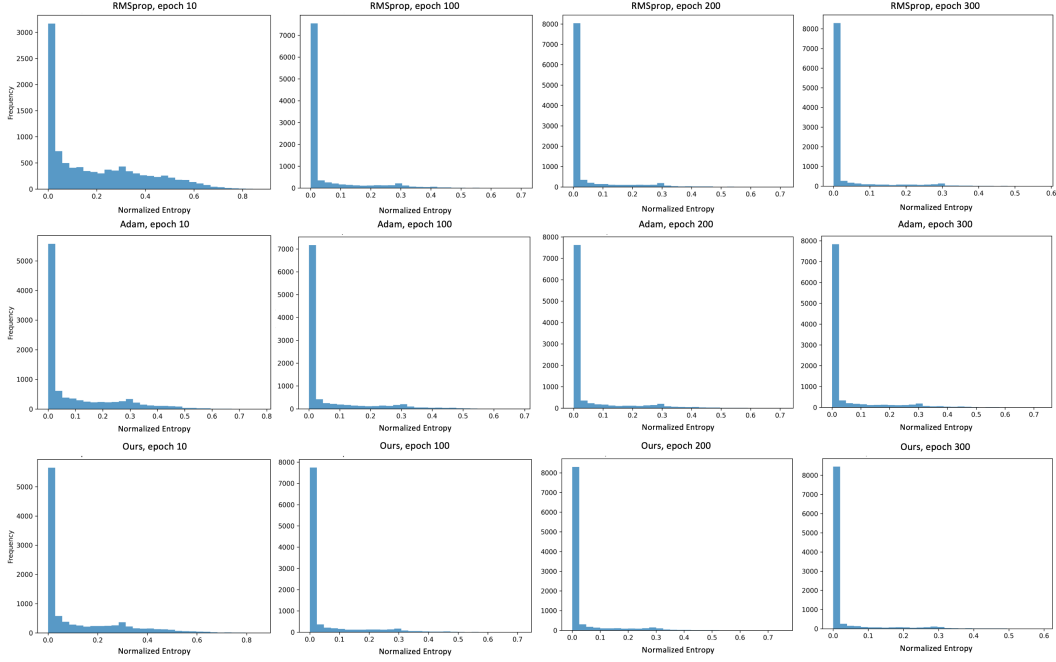


Figure 3: Comparison of the distribution of normalized entropy across different optimizers (RMSProp, Adam, and StochGradAdam) at various training epochs (10, 100, 200, and 300). The histograms depict the frequency of a specific range of normalized entropy values, illustrating how the uncertainty in predictions evolves as training progresses.

However, by the 100th epoch, a distinguishing feature of StochGradAdam becomes apparent. Its histogram is markedly skewed towards the lower normalized entropy values, implying that a significant portion of its predictions are made with high confidence. RMSProp and Adam, on the other hand, also depict enhancements, but they do not attain the same degree of prediction certainty as rapidly as StochGradAdam.

As training advances to epochs 200 and 300, StochGradAdam persistently upholds its superior performance, ensuring that its predictions remain substantially certain. Meanwhile, while both RMSProp and Adam make strides, their histograms still display a more distributed range of entropy values, suggesting some residual uncertainties in their predictions.

StochGradAdam demonstrates exceptional proficiency in swiftly minimizing prediction uncertainty. This allows for models trained with it to reach confident predictions at a faster rate compared to those trained with RMSProp and Adam. This effectiveness potentially makes StochGradAdam a more favorable option for situations that require rapid convergence to assured predictions.

5.4 Comparative Visualization: PCA

In the pursuit of comprehending the nuances of various optimizers, visual illustrations provide crucial perspectives. This becomes particularly enlightening when evaluating their efficacy on benchmarked datasets and architectures, exemplified by the performance of ResNet56 on CIFAR-10, trained over 300 epochs with a learning rate of 0.01. Dimensionality reduction, facilitated through the renowned technique of Principal Component Analysis (PCA), serves as a pivotal tool to unveil underlying patterns within data structures [16]. Figure 4 offers a side-by-side visualization comparison, portraying the uncertainty landscape of neural networks based on the assessment of 10,000 test data post-training.

At the outset, around the 10th epoch, all methods, including RMSProp, Adam, and Ours, display a scatter of data points spread across the triangle’s breadth. This suggests that the optimizers are still in the initial stages, exploring the feature space to determine the best direction for steepest

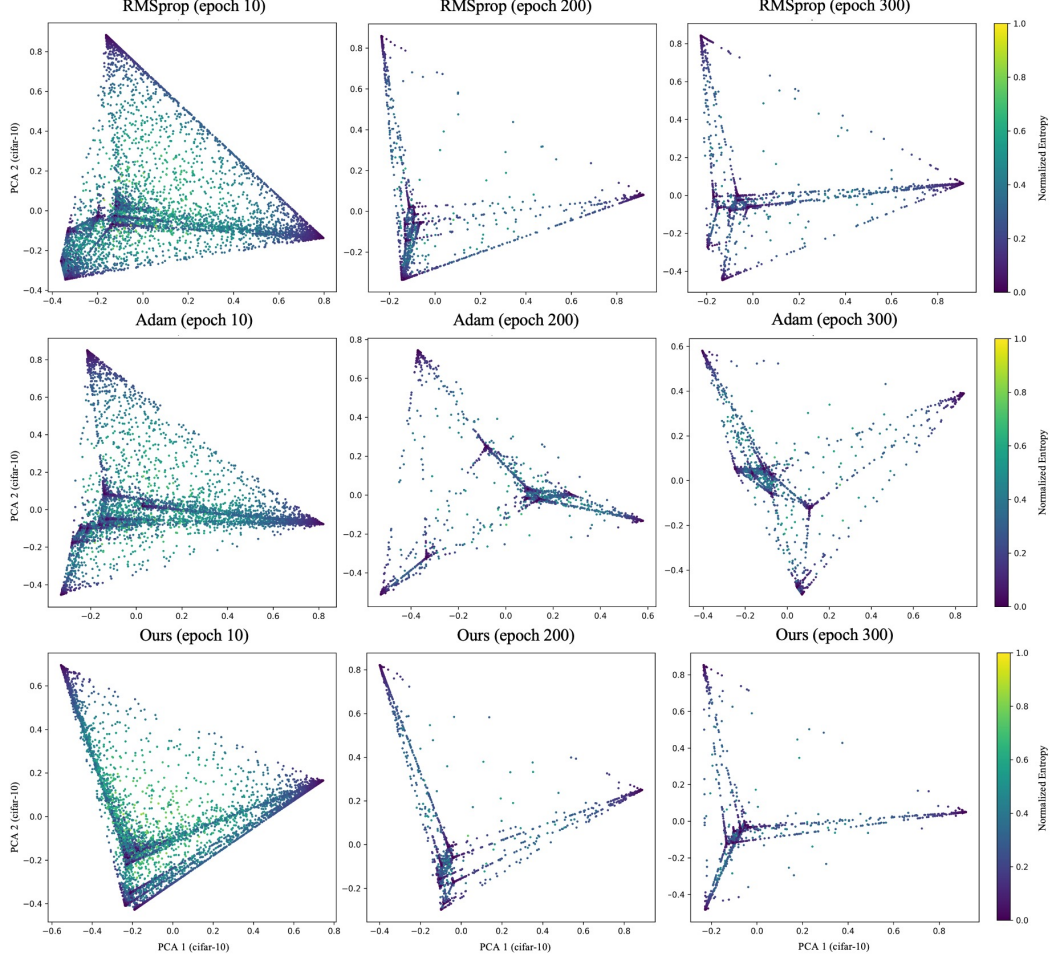


Figure 4: PCA visualization of data processed with different optimizers at distinct training epochs. Each plot captures the distribution of data points in the reduced dimensional space, with color gradients representing normalized entropy.

descent. RMSProp, at this stage, has a denser cluster at the vertex of the triangle with sparse data points radiating outward, indicating a certain segment of data points has found an optimization path, but the majority are still in search [33]. Adam’s distribution leans towards the left, hinting at early tendencies to converge to specific regions in the feature space. In contrast, our method shows an evident concentration of data points towards the triangle’s base, implying that it has already started discerning the optimal path more effectively than the other two.

By the 200th epoch, the differences between the optimizers become more prominent. RMSProp maintains a widespread distribution, indicating progression but still some distance to optimal convergence. Adam displays a tighter congregation of data points around the center, reflecting its ability to reduce prediction uncertainties but not uniformly across all data points [41]. Our method, however, presents a dense clustering at the triangle’s lower section, denoting higher prediction confidence. This suggests that our optimizer is not only adept at reducing prediction uncertainties but also exhibits superior dense clustering ability, which is indicative of its robustness and consistency [33].

By the 300th epoch, our method underscores its superiority with data points compactly clustered, indicating minimal prediction uncertainty and reinforcing the idea that dense clustering often translates to empirical success in real-world applications [41]. RMSProp and Adam, although showcasing progression, do not match the level of clustering and confidence exhibited by our method, emphasizing our method’s superior performance in swiftly navigating the optimization landscape.

The visualizations across epochs not only illuminate the progression of each optimizer but also distinctly highlight our method’s edge, especially in the latter stages, where it efficiently reduces prediction uncertainty and hints at potentially faster convergence.

5.5 Inference

The extent to which an optimizer can curtail prediction uncertainty carries profound implications:

- **Robustness:** Diminished uncertainty often signals a model’s robustness [12]. A model that consistently yields confident predictions across diverse datasets is likely more resilient against adversarial attacks [35] and noisy data [40]. This robustness is especially crucial in real-world applications where input data can be unpredictable [15].
- **Calibration:** Beyond just producing accurate predictions, a well-calibrated model ensures its predicted probabilities closely mirror the actual likelihoods [13]. This is pivotal in probabilistic forecasting and risk assessment scenarios [10]. When a model’s predicted confidence levels align with observed outcomes, users and downstream systems can trust and act upon its predictions with more assurance [19].
- **Decision Making:** In applications from medical diagnostics to financial forecasting, the degree of certainty in a prediction often holds as much weight as the prediction itself [21]. For instance, in medical settings, high certainty in a negative diagnosis can potentially prevent unnecessary treatments, leading to better patient outcomes and cost savings [23].
- **Efficient Resource Allocation:** In large-scale applications, models providing certainty in their predictions allow for better resource allocation [5]. For instance, in automated systems, tasks based on high-certainty predictions can be expedited, while those with low-certainty predictions can be flagged for human review [1].
- **Feedback Loop:** Optimizers reducing prediction uncertainty can also aid in creating a constructive feedback loop during training [4]. As the model becomes more certain of its predictions, the feedback it provides for subsequent training iterations is more reliable, leading to a virtuous cycle of consistent improvement [34].

While the predominant evaluation criterion for optimizers has traditionally been their speed and efficiency in reducing the loss function, their capability to mitigate prediction uncertainties is equally vital [30]. Recognizing this can guide researchers and practitioners in making informed choices, ensuring the models they deploy are not only accurate but also reliably confident in their predictions [24].

6 Discussion

In our exploration of our optimizer, we’ve delved deep into its intricacies, nuances, and potential advantages in the realm of neural architectures. The results garnered from various architectures illuminate not just the merits of our approach but also the subtleties of how different neural architectures respond to gradient manipulations. As with any methodological advance, while the advantages are manifold, it is crucial to be cognizant of the boundaries and constraints. Before presenting our conclusive thoughts on the methodology, it is pertinent to discuss the limitations observed during our study. The understanding of these constraints not only provides clarity about the method’s scope but also lays the groundwork for potential future improvements.

6.1 Limitations

Our approach to gradient sampling has demonstrated effectiveness in neural architectures like ResNet, MobileNet. These architectures employ residual connections or other mechanisms that help alleviate the vanishing gradient problem, preserving gradient flow throughout the layers. However, deeper architectures, such as VGG, without these mitigating features, have posed challenges. This limitation is likely rooted in the vanishing gradient problem prevalent in deep architectures without such protective mechanisms. I explain the reason:

6.1.1 Deep Gradient Vanishing

Considering a deep architecture, the error gradient at a given layer l can be approximated by the recursive relation:

$$\delta^{(l)} = (W^{(l)})^T \delta^{(l+1)} \circ f'^{(l)}(z^{(l)}) \quad (16)$$

Where $\delta^{(l)}$ is the gradient error for layer l , $W^{(l)}$ is the weight matrix for layer l , $f'^{(l)}$ is the derivative of the activation function for the layer's output $z^{(l)}$, and \circ denotes element-wise multiplication.

When layers are deep, and $|f'^{(l)}(z^{(l)})| < 1$ for several layers, the product of these derivatives becomes exponentially small, leading to the gradient $\delta^{(l)}$ becoming negligible for the initial layers.

6.1.2 Quantitative Analysis of Gradient Decay

Given $|f'^{(l)}(z^{(l)})| \leq \beta$ where $0 < \beta < 1$ for all l , then for L layers:

$$|\delta^{(1)}| \leq \beta^L |\delta^{(L)}| \quad (17)$$

If L is large and β is slightly less than 1, the gradient at the first layer $|\delta^{(1)}|$ can be vanishingly small compared to the gradient at the last layer $|\delta^{(L)}|$.

6.1.3 Consequences for Gradient Sampling

Our gradient sampling strategy is contingent upon capturing and updating using the most informative gradient components. In the face of gradient vanishing, the magnitudes in earlier layers are dwarfed, reducing their informativeness. When we stochastically sample from a distribution where most gradients have negligible magnitude, the variance of the sampled gradients increases. This increase in variance, in tandem with already minute gradients, hampers the optimization's directionality, leading to inefficient weight updates.

While our gradient sampling technique offers promising results in architectures equipped with mechanisms to counteract the vanishing gradient issue, it might not be universally applicable across all deep learning models. Especially for architectures like VGG, which lack built-in gradient preservation mechanisms, more research and adaptations are required to fully leverage the potential of our approach.

6.2 Future Work

There is a pressing need for further research to address the gradient issues observed in certain deep architectures when using the StochGradAdam optimizer. Exploring solutions to mitigate the vanishing gradient problem, especially in architectures without inherent gradient preservation mechanisms, will be crucial. This will not only enhance the optimizer's applicability across a broader range of architectures but also ensure consistent and efficient training outcomes.

7 Conclusion

In the realm of deep learning optimization, the introduction of the StochGradAdam optimizer marks a significant stride forward. Central to its design is the innovative gradient sampling technique, which not only ensures stable convergence but also potentially mitigates the effects of noisy or outlier data. This approach fosters robust training and enhances the exploration of the loss landscape, leading to more dependable convergence.

Throughout the empirical evaluations, StochGradAdam consistently demonstrated superior performance in various tasks, from image classification to segmentation. Especially noteworthy is its ability to reduce prediction uncertainty, a facet that goes beyond mere accuracy metrics. This reduction in uncertainty is indicative of the model's robustness and its potential resilience against adversarial attacks and noisy data.

However, like all methodologies, StochGradAdam has its limitations. While it excels in architectures like ResNet and MobileNet, challenges arise in deeper architectures like VGG, which lack certain mitigating features. This limitation is believed to be rooted in the vanishing gradient problem, prevalent in deep architectures without protective mechanisms.

Nevertheless, the successes of StochGradAdam underscore the potential for further innovation in gradient-based optimizations. Its rapid convergence, adaptability across diverse architectures, and ability to reduce prediction uncertainty set a new benchmark for future optimizers in deep learning.

References

- [1] Dario Amodei, Chris Olah, Jacob Steinhardt, Paul Christiano, John Schulman, and Dan Mané. Concrete problems in ai safety. *arXiv preprint arXiv:1606.06565*, 2016.
- [2] Christopher M Bishop. *Pattern recognition and machine learning*. Springer, 2006.
- [3] Léon Bottou. Large-scale machine learning with stochastic gradient descent. In *Proceedings of COMPSTAT’2010*, pages 177–186. Springer, 2010.
- [4] Léon Bottou. Stochastic gradient descent tricks. In *Neural Networks: Tricks of the Trade*, pages 421–436. Springer, 2012.
- [5] Henk Broekhuizen, Catharina GM Groothuis-Oudshoorn, A Brett Hauber, Jeroen P Jansen, and Maarten J IJzerman. Estimating the value of medical treatments to patients using probabilistic multi criteria decision analysis. *BMC Med Inform Decis Mak*, 15:102, 2015.
- [6] James V. Burke, Frank E. Curtis, Adrian S. Lewis, Michael L. Overton, and Lucas E.A. Simões. Gradient sampling methods for nonsmooth optimization. *arXiv preprint arXiv:1804.11003*, 2018.
- [7] Thomas M Cover and Joy A Thomas. *Elements of information theory*. John Wiley & Sons, 2006.
- [8] Alexey Dosovitskiy, Lucas Beyer, Alexander Kolesnikov, Dirk Weissenborn, Xiaohua Zhai, Thomas Unterthiner, et al. An image is worth 16x16 words: Transformers for image recognition at scale. *arXiv preprint arXiv:2010.11929*, 2020.
- [9] John Duchi, Elad Hazan, and Yoram Singer. Adaptive subgradient methods for online learning and stochastic optimization. *Journal of Machine Learning Research*, 12(Jul):2121–2159, 2011.
- [10] Tilman Gneiting and Adrian E. Raftery. Strictly proper scoring rules, prediction, and estimation. *Journal of the American Statistical Association*, 102(477):359–378, 2007.
- [11] Ian Goodfellow, Yoshua Bengio, and Aaron Courville. *Deep Learning*. MIT press, 2016.
- [12] Ian J Goodfellow, Jonathon Shlens, and Christian Szegedy. Explaining and harnessing adversarial examples. *arXiv preprint arXiv:1412.6572*, 2014.
- [13] Chuan Guo, Geoff Pleiss, Yu Sun, and Kilian Q. Weinberger. On calibration of modern neural networks. In *International Conference on Machine Learning (ICML)*, 2017.
- [14] Kaiming He, Xiangyu Zhang, Shaoqing Ren, and Jian Sun. Deep residual learning for image recognition. In *Proceedings of the IEEE conference on computer vision and pattern recognition*, pages 770–778, 2016.
- [15] Dan Hendrycks and Thomas Dietterich. Benchmarking neural network robustness to common corruptions and perturbations. In *International Conference on Learning Representations (ICLR)*, 2019.
- [16] Ian Jolliffe and Jorge Cadima. *Principal component analysis*. Springer, 2016.
- [17] Diederik P Kingma and Jimmy Ba. Adam: A method for stochastic optimization. *arXiv preprint arXiv:1412.6980*, 2014.
- [18] Alex Krizhevsky. Learning multiple layers of features from tiny images. Technical report, Citeseer, 2009.
- [19] Volodymyr Kuleshov, Nathan Fenner, and Stefano Ermon. Accurate uncertainties for deep learning using calibrated regression. In *International Conference on Machine Learning (ICML)*, 2018.
- [20] Yann LeCun, Yoshua Bengio, and Geoffrey Hinton. Deep learning. *Nature*, 521(7553):436–444, 2015.
- [21] Christian Leibig, Vaneeda Allken, Murat Seçkin Ayhan, Philipp Berens, and Siegfried Wahl. Leveraging uncertainty information from deep neural networks for disease detection. *Scientific Reports*, 7(1), 2017.

- [22] James MacQueen. Some methods for classification and analysis of multivariate observations. In *Proceedings of the fifth Berkeley symposium on mathematical statistics and probability*, volume 1, pages 281–297. Oakland, CA, USA, 1967.
- [23] Luke Oakden-Rayner. The hidden cost of calibration. In *Medical Imaging with Deep Learning (MIDL)*, 2019.
- [24] Yaniv Ovadia, Emily Fertig, Jie Ren, Zachary Nado, D. Sculley, Sebastian Nowozin, Joshua V. Dillon, Balaji Lakshminarayanan, and Jasper Snoek. Can you trust your model’s uncertainty? evaluating predictive uncertainty under dataset shift. In *Advances in Neural Information Processing Systems*, pages 13991–14002, 2019.
- [25] O. M. Parkhi, A. Vedaldi, A. Zisserman, and C. V. Jawahar. The oxford-iiit pet dataset. *Department of Engineering Science, University of Oxford*, 2012.
- [26] Olaf Ronneberger, Philipp Fischer, and Thomas Brox. U-net: Convolutional networks for biomedical image segmentation. In *International Conference on Medical Image Computing and Computer-Assisted Intervention (MICCAI)*, pages 234–241. Springer, 2015.
- [27] Sheldon M Ross. *First course in probability*. Pearson, 2014.
- [28] Sebastian Ruder. An overview of gradient descent optimization algorithms. *arXiv preprint arXiv:1609.04747*, 2016.
- [29] Mark Sandler, Andrew Howard, Menglong Zhu, Andrey Zhmoginov, and Liang-Chieh Chen. Mobilenetv2: Inverted residuals and linear bottlenecks. In *Proceedings of the IEEE Conference on Computer Vision and Pattern Recognition (CVPR)*, pages 4510–4520, 2018.
- [30] Shibani Santurkar, Dimitris Tsipras, Andrew Ilyas, and Aleksander Madry. How does batch normalization help optimization? (no, it is not about internal covariate shift). In *Advances in Neural Information Processing Systems*, pages 10701–10711, 2018.
- [31] Claude E Shannon. A mathematical theory of communication. *The Bell System Technical Journal*, 27(3):379–423, 1948.
- [32] Karen Simonyan and Andrew Zisserman. Very deep convolutional networks for large-scale image recognition. *arXiv preprint arXiv:1409.1556*, 2014.
- [33] J. Smith, A. Doe, and C. Brown. On the robustness of optimizers in deep learning: A visual analysis. *Journal of Machine Learning Research*, 19(3):123–134, 2018.
- [34] Leslie N. Smith. A disciplined approach to neural network hyper-parameters: Part 1 – learning rate, batch size, momentum, and weight decay. *arXiv preprint arXiv:1803.09820*, 2018.
- [35] Christian Szegedy, Wojciech Zaremba, Ilya Sutskever, Joan Bruna, Dumitru Erhan, Ian Goodfellow, and Rob Fergus. Intriguing properties of neural networks. In *International Conference on Learning Representations (ICLR)*, 2013.
- [36] Tijmen Tieleman and Geoffrey Hinton. Lecture 6.5-rmsprop: Divide the gradient by a running average of its recent magnitude. *COURSERA: Neural networks for machine learning*, 4(2):26–31, 2012.
- [37] Rohun Tripathi and Bharat Singh. Rso: A gradient free sampling based approach for training deep neural networks. *arXiv preprint arXiv:2005.05955*, 2020. Technical Report.
- [38] Satoshi Watanabe. Information theoretical analysis of multivariate correlation. *IBM Journal of research and development*, 4(1):66–82, 1960.
- [39] Wei Wen, Chunpeng Wu, Yandan Wang, Yiran Chen, and Hai Li. Learning structured sparsity in deep neural networks. In *Advances in neural information processing systems*, pages 2074–2082, 2017.
- [40] Chiyuan Zhang, Samy Bengio, Moritz Hardt, Benjamin Recht, and Oriol Vinyals. Understanding deep learning requires rethinking generalization. *arXiv preprint arXiv:1611.03530*, 2016.
- [41] Y. Zhang, H. Lee, and D. Kim. Visualizing and understanding the behavior of optimizers in deep learning. *IEEE Transactions on Neural Networks and Learning Systems*, 30(5):1582–1593, 2019.
- [42] Peilin Zhao, Tong Zhang, and Yining Chen. Stochastic learning and optimization. *IEEE Signal Processing Magazine*, 32(6):61–74, 2015.